Published in final edited form as:
Brain Res. 2011 September 21; 1413: 9–23. doi:10.1016/j.brainres.2011.06.066.

The Role of Mesopontine NGF in Sleep and Wakefulness

Oscar V. Ramos[2], **Pablo Torterolo**[4], **Vincent Lim**[2], **Michael H. Chase**[2,3], **Sharon Sampogna**[2], and **Jack Yamuy**[1]

[1]VA Greater Los Angeles Healthcare System, Los Angeles, CA, 90073

[2]Websciences International, Los Angeles, CA, 90024

[3]UCLA School of Medicine Los Angeles, CA, 90024

[4]Departamento de Fisiología, Facultad de Medicina, Universidad de la República, Montevideo, Uruguay

Abstract

The microinjection of nerve growth factor (NGF) into the cat pontine tegmentum rapidly induces rapid eye movement (REM) sleep. To determine if NGF is involved in naturally-occurring REM sleep, we examined whether it is present in mesopontine cholinergic structures that promote the initiation of REM sleep, and whether the blockade of NGF production in these structures suppresses REM sleep. We found that cholinergic neurons in the cat dorsolateral mesopontine tegmentum exhibited NGF-like immunoreactivity. In addition, the microinjection of an oligodeoxyribonucleotide (OD) directed against cat NGF mRNA into this region resulted in a reduction in the time spent in REM sleep in conjunction with an increase in the time spent in wakefulness. Sleep and wakefulness returned to baseline conditions 2 to 5 days after antisense OD administration. The preceding antisense OD-induced effects occurred in conjunction with the suppression of NGF-like immunoreactivity within the site of antisense OD injection. These data support the hypothesis that NGF is involved in the modulation of naturally-occurring sleep and wakefulness.

Keywords

Neurotrophin; brainstem; reticular formation; LDT; PPT; immunohistochemistry

1. Introduction

The ponto-mesencephalic junction contains structures that are responsible for the control of behavioral states (Jones, 2005; Siegel, 2005; McCarley, 2007). Ascending and descending projections arising from this reticular region play a key role in the regulation of cortical and motor activity (Mitani et al., 1988; Pare et al., 1988; Jones, 1990; Semba et al., 1990; Shiromani et al., 1990). A large population of cholinergic neurons in the latero-dorsal and pedunculo-pontine tegmental nuclei (LDT and PPT), that are located in the dorso-medial and dorso-lateral aspects of the mesopontine tegmentum, are thought to be critical for the

Corresponding author: Jack Yamuy, M.D., VA Greater Los Angeles Healthcare System, Los Angeles, CA 90073, Tel: 310-384-2091, jyamuy@ucla.edu.

control of REM sleep and wakefulness (Jones, 2005; Siegel, 2005; McCarley, 2007). These cholinergic cells project ventrocaudally to the adjacent nucleus pontis oralis (NPO), which contains neurons that are involved in the execution of the typical phenomena of REM sleep, as well as rostrally to the thalamus and hypothalamus (ibid.).

It has been unambiguously demonstrated that neurotrophins, in addition to their trophic actions, are capable of acting both pre- and postsynaptically as modulators of neuronal activity (Lohof et al., 1993; Knipper et al., 1994; Shen et al., 1994). In this regard, we have reported that the microinjection of nerve growth factor (NGF) into the NPO of the cat rapidly induces a state that, except for its long duration, is indistinguishable from naturally-occurring REM sleep (Yamuy et al., 1995a). In addition, the NGF-induced REM sleep-like state is mediated by tropomyosin-related kinase A (trkA) which binds with high affinity to NGF and, to a lesser extent, to neurotrophin-3 (Yamuy et al., 2005).

Based upon the aforementioned data, we hypothesized that NGF acts as an endogenous neuromodulator to promote the generation of naturally-occurring REM sleep. To confirm this hypothesis, it is first necessary to demonstrate the existence of a source of NGF in structures that are involved in the generation of REM sleep and, additionally, that a decrease in the production of NGF at the source results in a reduction of the time spent in this behavioral state. In the present study, we tested if cholinergic neurons in the LDT-PPT exhibit NGF-like immunoreactivity and, additionally, we used local antisense microinjections to block NGF synthesis in these nuclei. The data that were obtained lend credence to our hypothesis, i.e., cholinergic neurons within the LDT-PPT show NGF-like immunoreactivity and the antisense-induced blockade of NGF mRNA in the LDT-PPT significantly reduces the occurrence of REM sleep.

2. Results

2.1. NGF immunoreactivity in the LDT and PPT

In order to test the hypothesis that NGF acts as an endogenous modulator of REM sleep, we first asked whether neurons in the LDT-PPT of the cat contained NGF. For this purpose, we conducted a qualitative determination of NGF immunoreactivity in these structures. We found that NGF-like immunoreactivity was present in neurons of the LDT-PPT at all of the mesopontine levels that were examined. This result is illustrated in Fig. 1A-D for both the LDT and PPT. Several control methods were used to establish the specificity of NGF immunostaining. First, the omission of the primary antibody yielded sections that were devoid of NGF-like immunostaining. Second, NGF-like immunoreactivity was suppressed following the adsorption of the primary antibody with either a specific control peptide (Santa Cruz Biotechnol., CA) or an NGF extract from the mouse submaxillary gland (Santa Cruz Biotechnol., CA). Third, whereas the microinjection of human recombinant NGF (Santa Cruz Biotechnol., CA) into the pontine tegmentum yielded strong NGF-like immunostaining, pontine sections in which the primary antibody was adsorbed by a saturating concentration of a specific control peptide provided by the manufacturer, a mouse NGF extracted from the submaxillary gland, or a human recombinant NGF, did not show NGF-like immunoreactivity (data not shown). Finally, the NGF primary antibodies that were used in the present study marked cells in brainstem nuclei that are known to contain NGF immunoreactive neurons, i.e., the cochlear, vestibular, and mesencephalic trigeminal nuclei (see below) (Nishio et al., 1994; Jacobs and Miller, 1999).

Whereas neurons of diverse phenotypes are known to be present in the LDT-PPT (Clements and Grant, 1990; Jones, 1990; Torterolo et al., 2001; Jia et al., 2003), we were interested in determining whether the subpopulation of cholinergic neurons in the LDT-PPT contained NGF, i.e., were NGF immunoreactive. Data obtained from double-labeling studies showed

that LDT-PPT cells that were immunostained for choline acetyltransferase (ChAT), the synthetic enzyme for acetylcholine and a specific marker of cholinergic cells, also exhibited NGF-like immunoreactivity; this result is illustrated in Fig. 2, wherein all of the ChAT-containing neurons in the LDT (A and B) showed NGF-like immunostaining (C and D). On the other hand, it is important to note that not all of the NGF-like immunoreactive neurons in the LDT-PPT were ChAT immunostained. This is illustrated in Fig. 2 wherein neurons that exhibited clear NGF-like immunostaining were devoid of ChAT (arrowheads in Fig. 2A and D for the LDT, and arrowhead in Fig. 2C and F for the PPT). Although quantitative determinations were not conducted in the present study, these data indicate that a portion of NGF immunoreactive LDT-PPT neurons is non-cholinergic. These NGF single-labeled cells were medium- to large-sized and multipolar or fusiform in shape (arrowheads in Fig. 2D and F).

2.2. Alterations in the architecture of the states of sleep and wakefulness

To block NGF production in the LDT-PPT nuclei, an antisense oligodeoxyribonucleotide (OD) directed against cat NGF mRNA was microinjected into the LDT-PPT. The use of antisense has been shown to be valuable in revealing the functional role of proteins in behavior (Thakkar et al., 1999; Xi et al., 1999; Thakkar et al., 2003).

The microinjection site, a representative animal is shown in Figure 3; the injection was located in the caudo-ventral PPT. The effects of the microinjection of the control and antisense ODs in this cat are presented in Fig. 4. The percentage of time spent in REM sleep during the days of injection of the control OD (indicated by the bar in the abscissa, upper chart in Fig. 4A) was similar to that present during baseline sessions prior to and following the control OD series of injections. In contrast, a decrease in the percentage of time spent in REM sleep occurred during the microinjections of the antisense OD (indicated by the bar in the abscissa, lower chart in Fig. 4A). This change was first detected during the second antisense OD recording session, i.e., 24 hours after the beginning of the NGF antisense series of microinjections. The maximum decrease in the time spent in REM sleep was reached more than 48 hours after the initial application of the antisense OD; it amounted to a 65% reduction compared to baseline levels (lower chart in Fig. 4A). The percentage of time spent in REM sleep was maintained, during a period of five days after the last antisense injection, at levels lower than those of baseline sessions (Fig. 4A; this period lasted between 2-5 days in different cats). Note that in the fifth antisense session, REM sleep returned to a level similar to that exhibited during baseline sessions. As illustrated in Fig. 4, the time spent in REM sleep was reduced in the subsequent three days. Figure 4A also illustrates that changes were not restricted to REM sleep. In conjunction with the decrease in the time spent in REM sleep, there was an increase in the time spent in wakefulness (maximum increase, 78%) as well as a decrease in the time spent in NREM sleep (maximum decrease, 50%) during the antisense OD series of injections (lower chart in Fig. 4A).

Hypnograms from the same animal that were constructed from a representative baseline session and the third day of control and antisense OD injection sessions are presented in Fig. 4B. Whereas during baseline and control OD sessions similar patterns of distribution of episodes of sleep and wakefulness occurred, in the antisense OD session there was a decrease in REM sleep and an increase in wakefulness (lower hypnogram in Fig. 4B). These changes were particularly evident during the second half of the recording session.

Similar changes in the architecture of sleep and wakefulness were observed in all antisense OD-injected animals. The mean percentages of time spent in sleep and wakefulness observed in each animal during antisense OD sessions, compared to those obtained during baseline sessions, are depicted in Fig. 5A. Note that in one cat there was a slight decrease in wakefulness (experiment identified by triangles in Fig. 5A, left-hand bar chart), and in two

cats there was an increase in NREM sleep (experiments indicated by triangles and diamonds in Fig. 5A, middle bar chart). In contrast, the microinjection of antisense OD was consistently followed by a decrease in REM sleep in all animals (Fig. 5A, right-hand bar chart).

Although the injection procedures were exactly the same, paired comparison of the data obtained following microinjections of control OD and antisense OD in three cats (empty and solid bars in Fig. 5B, respectively), wherein each cat serves as its own control, revealed that there was a statistically significant difference in the mean percentage of time spent in wakefulness, NREM sleep, and REM sleep (Fig. 5B).

Multifactorial analyses of variance (ANOVA) accompanied by the Scheffé *post hoc* test were conducted using the pooled data obtained from all the animals for each treatment. These analyses confirmed the existence of significant differences in the means for the percentage of time spent in wakefulness, NREM sleep, and REM sleep during baseline and control antisense sessions compared with those obtained during antisense sessions (Table 1).

It is important to note that, because all of the antisense OD injection days were systematically selected for the foregoing statistical analyses, the changes in the mean percentage of time spent in sleep and wakefulness are underestimated. Indeed, there were no evident behavioral state alterations during the first antisense OD injection day, and recovery to baseline levels were observed during the latter antisense OD injection days. This conservative approach was used in order to avoid the possibility of a biased selection of experimental data and strengthen the obtained results.

No significant differences in the means of the measured variables were present when baseline sessions were compared to those in which the control OD was injected (Table 1).

Finally, in the two animals in which a second series of antisense OD injections were performed, a decrease in REM sleep time was observed as in the first antisense OD microinjection series. This decrease in REM sleep time was accompanied by a decrease in NGF-like immunoreactivity (see below).

2.3. Latency to the onset of sleep states

All of the microinjections of ODs were conducted while the cats were awake. Therefore, we examined whether the latencies to the onset of NREM and REM sleep were altered during antisense OD recording sessions. Hence, the mean latency to the onset of REM sleep was significantly longer during antisense sessions than during baseline and control antisense sessions (Table 1). In addition, similar analyses revealed that the latency to the onset of NREM sleep during NGF antisense OD sessions was significantly longer than that during baseline sessions, but did not reach statistical significance against the control OD sessions (Table 1).

2.4. Frequency and duration of episodes of sleep and wakefulness

The changes in the time spent in the states of sleep and wakefulness that were present following the administration of NGF antisense could have been due to alterations in the frequency and/or duration of individual episodes of each behavioral state. The analysis revealed that there was a statistically significant reduction in the mean frequency of REM sleep episodes during antisense OD sessions compared to baseline and control OD sessions (Table 1). Furthermore, there were no statistically significant changes in the mean frequency of wakefulness and NREM sleep episodes. In addition, there was a statistically significant increase in the mean duration of wakefulness episodes during antisense OD sessions compared with baseline and control OD sessions. On the other hand, there were no

statistically significant changes in the mean duration of NREM and REM sleep episodes (Table 1). Thus, significant changes in the frequency or duration of episodes were confined to REM sleep and wakefulness. This is consistent with the concept that the injected antisense OD acted on cells in a region, i.e., the LDT-PPT, that is specifically involved in the control of REM sleep and wakefulness (Webster and Jones, 1988; Steriade et al., 1990; Datta et al., 2001; Jones, 2005).

2.5. Patterns of EEG activity that characterize sleep and wakefulness

Because the microinjection of NGF antisense was followed by changes in the architecture of sleep and wakefulness, we sought to determine whether these changes were correlated with alterations in the frequency components of the electroencephalogram (EEG). Typically, an activated EEG (low-amplitude, high-frequency wave patterns) is present during wakefulness and REM sleep, whereas a synchronized EEG (high-amplitude, low-frequency wave patterns) occurs during NREM sleep, i.e., different frequency bands are known to be predominant during each state of vigilance (Steriade, 2005).

No major changes in the frontal and parietal EEG, electro-oculogram (EOG), electrogram of the lateral geniculate nucleus (LGN) or electromyogram (EMG) were observed by visual inspection after the microinjection series, neither during wakefulness nor during sleep. In Fig. 6 the distribution of the power for frequencies between 0 and 60 Hz of the frontal EEG is illustrated for quiet wakefulness, deep NREM sleep, and REM sleep. These line charts show that the power spectra for each behavioral state were similar for baseline, control and NGF antisense sessions.

2.6. NGF-like immunoreactivity in the LDT-PPT following the microinjection of NGF antisense

To verify that the behavioral effects of the antisense OD occurred as a consequence of a decrease in the levels of NGF in the LDT-PPT, we examined whether NGF-like immunoreactivity changed in these structures in cats that were euthanized during the peak of the antisense-induced behavioral effects. Data obtained from triple-labeling experiments are illustrated in the photomicrographs in Fig. 7. The region of antisense OD application was marked, with an injection of the control antisense OD that was tagged with fluorescein isothiocyanate (FITC); microvessels, glial cells and the profile of neurons that took up the tagged control OD are shown in Fig. 7A (neurons are indicated by arrows). As described by others, the neurons that took up the OD exhibited FITC fluorescence within their cytoplasm and nucleus (Leonetti et al., 1991; Thakkar et al., 2003). The presence of cholinergic neurons in the same region of the LDT is illustrated in Fig. 7B; note that these are typical medium- to large-sized, ChAT-containing neurons and that they are also immunofluorescent for the tagged OD (merged image in Fig. 7C). The identical region of the LDT is depicted under bright field microscopy in order to visualize NGF immunoreactivity (Fig. 7D); the neuronal profiles are empty or difficult to distinguish from the background indicating that NGF immunoreactivity was virtually absent. Thus, in contrast with the suppression of NGF immunostaining, ChAT immunoreactivity was intact in cholinergic LDT-PPT neurons and, in addition, these cholinergic cells appeared to be normal in size and morphology.

In order to determine that the antisense OD-induced blockade of NGF synthesis was site specific, we examined if NGF immunostained neurons were present in brainstem regions that were not exposed to the injected NGF antisense. Whereas NGF immunoreactivity was suppressed within the boundaries of the antisense OD injection (Fig. 8A-C), neurons in the mesencephalic trigeminal, cochlear, and vestibular nuclei exhibited clear NGF immunoreactivity (Fig. 8D-F); these nuclei have been shown to contain NGF immunoreactive neurons (Nishio et al., 1994; Jacobs and Miller, 1999). Furthermore, it is

important to note that, based on both tagged OD and NGF immunoreactivities, the injections of the NGF antisense did not reach the LDT-PPT in their entirety. As shown in Fig. 9A-D, areas in these nuclei that were adjacent to the injection site were devoid of NGF immunoreactivity, whereas distant regions exhibited NGF immunolabeled neurons.

3. Discussion

Three fundamental results are reported in the present study. First, NGF-like immunoreactivity is present in neurons in the cat LDT-PPT, including the large population of cholinergic cells involved in the control of wakefulness and REM sleep (Jones, 2005). Second, the application of an antisense OD directed against cat NGF mRNA into the LDT-PPT is followed by a decrease in REM sleep and an increase in wakefulness. Third, the antisense OD-induced alterations in the architecture of the sleep-wake cycle are associated with a selective decrease in NGF-like immunoreactivity in LDT-PPT cells. Taken together, these results provide evidence that NGF in LDT-PPT neurons is involved in the control of naturally-occurring REM sleep and wakefulness.

3.1. Alterations in the states of sleep and wakefulness following the microinjection of antisense OD

The time spent in REM sleep as well as the frequency of REM sleep episodes were significantly reduced, and the latency to the onset of this state increased, following antisense OD administration; nevertheless the duration of the REM sleep episodes were not modified. These results agree with our hypothesis that NGF acts to enhance naturally-occurring REM sleep (Yamuy et al., 1995a). However, the effect of antisense was not selective for this behavioral state, i.e., the frequency of the episodes, and time spent in wakefulness increased, while the latency and time spent in NREM sleep decreased. Therefore, our results raise the question of how a deficit in NGF in LDT-PPT neurons could have promoted changes in wakefulness, REM sleep and, to a lesser extent, NREM sleep.

An antisense OD-induced non-specific effect on the sleep-wake cycle is unlikely because the randomized OD, injected under identical conditions, did not produce behavioral state changes. Furthermore, the antisense OD elicited changes predominantly in wakefulness and REM sleep. This is consistent with the fact that neurons in the LDT-PPT, an arm of the ascending reticular activating system (ARAS), are involved in the control of both of these behavioral states (Steriade, 1996; Skinner et al., 2004; Jones, 2005; Torterolo and Vanini, 2010). These nuclei contain cholinergic and non-cholinergic cells that are active during wakefulness and/or REM sleep and project rostrally to thalamic and hypothalamic regions where they excite neurons that are responsible for activating the EEG (Hallanger and Wainer, 1988; Steriade et al., 1990; Semba and Fibiger, 1992). In addition, a subpopulation of cholinergic cells in the LDT-PPT are active during REM sleep and project to the NPO (Webster and Jones, 1988; Jones, 1990; Semba and Fibiger, 1992). The small decrease in NREM sleep (12%) is likely a consequence of the large increase in wakefulness induced by the injection of the antisense OD into an area that is known to be a part of ARAS.

The antisense and control ODs were microinjected, at the same time of day, on successive days. Therefore, circadian factors that could influence the action of the drug were minimized. In addition, the antisense OD induced changes in sleep and wakefulness became evident between 24 and 72 hours after the first injection. These results indicate that the manipulation procedures, *per se*, did not contribute to the changes in behavioral states. Rather, based upon studies that have examined the antisense-induced blockade of other gene protein products (Wahlestedt et al., 1993; Barclay et al., 2002; Ettaiche et al., 2006), this period of time is consistent with a blocking action at the translational level of protein

synthesis plus the time required for depleting NGF in axons and synaptic terminals of LDT-PPT cells (Heumann et al., 1984; Ure and Campenot, 1997).

Data in the literature show the existence of NGF-induced modulatory actions on cholinergic synapses (Sala et al., 1998; Auld et al., 2001). We have recently obtained preliminary data that indicate that NGF acts presynaptically to enhance the muscarinic postsynaptic excitation of NPO neurons in the rat (Yamuy et al., 2004; Yamuy et al., 2005). Thus, the decrease in REM sleep is probably due to an antisense OD-induced deficit in the content of NGF in LDT-PPT synaptic terminals that impinge on NPO REM-on neurons. However, cholinergic LDT-PPT projections to the thalamus are excitatory and activate the EEG (Curro Dossi et al., 1991; Steriade et al., 1991a; Steriade et al., 1991b). If NGF acts in a similar manner in all LDT-PPT cholinergic synapses, opposite antisense-induced effects should have been observed, i.e., excitatory projections from the LDT-PPT to thalamic and hypothalamic neurons would be expected to be less effective following the antisense OD-induced deficit in NGF, thus resulting in a decrease in wakefulness. In spite of this, it is important to note that cholinergic LDT-PPT neurons exhibit a powerful muscarinic autoinhibitory effect through recurrent axon collaterals (el Mansari et al., 1990; Leonard and Llinas, 1994). It is possible that, by also decreasing the autoinhibition of wake-on cholinergic neurons, the net result of the antisense OD-induced deficit in NGF is an enhanced drive for wakefulness. Notwithstanding the speculative nature regarding the antisense OD mechanisms of action, the results indicate that this neurotrophin exerts a modulatory effect that enhances REM sleep and reduces wakefulness.

3.2. Patterns of EEG electrical activity following the microinjection of antisense OD

The power spectrum of the frontal EEG following antisense OD injections was similar to those obtained during baseline and control OD sessions. Animals that are deprived of NREM sleep exhibit increased slow wave activity (SWA; delta frequency band, between 0.5 and 4 Hz) that reflects augmented sleep pressure (Borbely, 1982). The absence of an increased SWA during antisense treatment agrees with the observation that the decrease in NREM sleep was minimal following the administration of antisense OD. In spite of the antisense-induced changes in the amount of wakefulness and REM sleep, the lack of changes in the frequency components of the EEG during these states suggests that the behavioral state-specific patterns of electrical activity of neurons that are critical for EEG activation remained unchanged.

3.3. NGF-like immunoreactivity in the LDT and PPT

A large population of LDT-PPT neurons exhibited NGF-like immunoreactivity in naïve animals; whereas we did not attempt to conduct quantitative analyses, it is likely that most of these NGF-like immunoreactive neurons were cholinergic, i.e., contained ChAT. These data indicate that there is an endogenous source of NGF in the LDT-PPT of the cat and that this neurotrophin plays a role in the mesopontine neurons that are involved in the control of REM sleep and wakefulness (Jones, 2004; McCarley, 2004). Recently, we reported that another neurotrophin, neurotrophin 3 (NT-3), was also present in LDT-PPT cholinergic cells (Yamuy et al., 2002). It is possible that these neurotrophins provide a trophic support to the LDT-PPT cells in the cat. Another possibility is that NGF is involved in mechanisms of synaptic modulation of neuronal activity. In favor of this hypothesis, the local application of the antisense OD was followed by a suppression of NGF-like immunoreactivity and clear changes in sleep and wakefulness; no degradative changes in cholinergic LDT-PPT cells, indicative of trophic alterations, were detected. These results are in agreement with the large body of evidence that demonstrates that neurotrophins, including NGF, act as neuromodulators of neuronal activity in the adult central and peripheral nervous systems (Lohof et al., 1993; Shen et al., 1994; Wang et al., 2002; Luther and Birren, 2006).

Several reasons support the concept that the immunostaining obtained in cat brain tissue was specific for NGF. First, we employed two different antibodies which have been reported to specifically immunostain for NGF (Quartu et al., 1997; Kawai et al., 2002; Quartu et al., 2003); both yielded similar qualitative results. Second, we carried out control experiments in order to confirm the specificity of NGF immunoreactivity, including a) the omission of the primary antibody suppressed or greatly attenuated NGF immunoreactivity, b) preadsorption of the primary antibody using mouse NGF, human NGF, and a specific peptide provided by the manufacturer suppressed NGF immunoreactivity, and c) immunohistochemistry for NGF in pontine sections that were obtained from a cat that was injected with human recombinant NGF into the pontine reticular formation yielded a strong NGF signal in the site of injection. Third, we confirmed, in the cat, the presence of NGF-like immunostained neurons in nuclei that have been previously reported to exhibit NGF immunoreactivity, i.e., the mesencephalic trigeminal, cochlear and vestibular nuclei (Nishio et al., 1994; Jacobs and Miller, 1999). Fourth, the site of injection of antisense OD in the LDT-PPT was devoid of NGF immunoreactive cells, whereas the LDT-PPT, in more distant regions, contained cholinergic cells that exhibited NGF immunoreactive neurons. Therefore, the results of these experiments lend credence to the concept that the primary antibodies used in the present study specifically bound to endogenous NGF.

Because the antisense OD did not diffuse into distant structures in the brainstem, the source of NGF is expected to be local to the site of injection. However, we can't discard that the antisense OD reach sleep-related areas in the vicinity of the PPT, specially the NPO.

Therefore, the presence of NGF-like immunoreactivity in neurons in the LDT-PPT suggests that these neurons are capable of synthesizing this neurotrophin. However, the use of techniques that reveal the existence of NGF mRNA, i.e., in situ hybridization, is necessary to prove that NGF is actually produced in LDT-PPT cholinergic cells.

Previous studies in rodents have reported that NGF was present in mesopontine areas only during development and that cultured PPT cholinergic cells were devoid of and unresponsive to NGF (Knusel and Hefti, 1988; Maisonpierre et al., 1990; Lauterborn et al., 1994). Differences in the experimental design and/or the species used in our studies may be responsible for these discrepancies. In fact, there are data that suggest that the mesopontine REM sleep generating mechanism differ in rodents and cats (Fuller et al., 2007; Luppi et al., 2007; McCarley, 2007).

3.4. NGF immunoreactivity in the LDT-PPT following the microinjection of antisense OD

The reversibility of antisense OD-induced effects on sleep and wakefulness and the lack of effect of the control, randomized OD demonstrate that the antisense treatment was not toxic to neurons in the LDT-PPT. To determine the antisense OD effectiveness and specificity in blocking the synthesis of NGF, immunohistochemical studies were carried out in cats that were euthanized during antisense treatment. These experiments revealed that NGF immunoreactivity in the LDT-PPT was suppressed or decreased compared to that observed in naïve cats. Notwithstanding the changes in NGF-like immunoreactivity levels in cholinergic cells in the LDT-PPT, these neurons maintained their normal shape and size, and their ChAT immunostaining was qualitatively intact. These data confirm that the antisense OD was not deleterious and produced a specific decrease in NGF. However, the antisense OD did not induce a total suppression of REM sleep. This was likely due to the fact that the drug reached only a portion of neurons in the LDT-PPT; it is virtually impossible to affect in its entirety such a large and irregularly shaped structure.

3.5. Conclusions

The present results reveal that the antisense-induced blockade of NGF synthesis in the LDT-PPT in the cat produces significant alterations in REM sleep and wakefulness. These data provide physiologic significance to our previous reports that showed that the application of NGF into the NPO induces REM sleep via its binding to trk receptors present in neurons and axon terminals in this nucleus (Yamuy et al., 1995a; Yamuy et al., 2000; Yamuy et al., 2002; Yamuy et al., 2005). Taken together, our results support the hypothesis that NGF acts as an endogenous modulator in the mechanisms responsible for the generation of naturally-occurring REM sleep and the suppression of wakefulness. Further investigation is necessary to confirm whether the cellular source of NGF synthesis are the LDT-PPT cholinergic neurons and the subcellular mechanisms whereby this neurotrophinergic system exerts its influence in the control of REM sleep and wakefulness.

4. Experimental procedure

A total of eight adult cats were used in the present study. Five of these animals were used in experiments aimed at determining the behavioral effects of antisense injections into the LDT-PPT; two of the foregoing experimental cats and three naïve animals were used for immunohistochemical studies. All cats were in good health, throughout the experiments, as determined by veterinarians in the Department of Laboratory Medicine of UCLA School of Medicine. Efforts were made to use a minimal number of animals and the experimental procedures that were employed were in accord with the guidelines set forth in the Guide for the Care and Use of Laboratory Animals, National Research Council (1996).

4.1. Surgical procedures

Details of the preparation of cats for monitoring behavioral states and microinjecting drugs into the rostral pontine tegmentum have been previously reported (Yamuy et al., 1993; Yamuy et al., 1995a; Yamuy et al., 2002). Under isoflurane anesthesia, screw electrodes were placed in the calvarium for the recording of the frontal and parietal EEG and in the orbital bone for the recording of the EOG; strut electrodes were directed stereotaxically to the LGN in order to examine ponto-geniculo-occipital (PGO) waves. All electrodes were connected to a female Winchester plug. Two plastic tubes, which were used to maintain the animal's head in a stereotaxic position without pain or pressure as well as the Winchester plug were fixed to the skull with acrylic resin. A 5-mm diameter hole was trephined overlying the posterior fossa in order to provide access for a cannula for drug microinjection. The hole was covered with a sterile bonewax plug. At the completion of surgery, antibiotics were administered parenterally for three days. The skin margins surrounding the implant were kept clean and topical antibiotics were administered on a daily basis.

4.2. Antisense against cat NGF mRNA

To block the synthesis of NGF, we used a phosphorothioated antisense oligodeoxyribonucleotide (OD) directed to cat NGF mRNA; phosphorothioated ODs have an increased resistance to exo- and endonucleases, are less toxic and highly soluble. A randomized phosphorothioated OD was used as control. In addition, a fluorescein-labeled, randomized, phosphorothioated control OD was used to determine the uptake of the ODs by neurons in the LDT-PPT and the site of OD injection within the ponto-mesencephalic junction. The ODs were designed and manufactured by Biognostik® (Göttingen, Germany). The sequences of these ODs were as follows: a) antisense NGF, 5′ - GTG AAC AGC ACG CG - 3′, which targets bases 37-50 of the NGF mRNA total sequence; b) randomized control

antisense, 5′ - ACT ACT ACA CTA GAC TAC - 3′; and c) FITC labeled randomized control antisense, 5′ - GTC CCT ATA CGA CC - 3′.

4.3. Recording and antisense injection procedures

The cats were adapted to the head restraining device (Model 880, David Kopf, CA) for at least two weeks. During the recording sessions, the animals were placed into a sound-attenuated box (approximately 1 m^3 in volume) with a one-way viewing window. The box was maintained at a temperature of 23 °C with lights on. Two stainless steel wires, insulated except for 1 mm at their tips, were inserted into the posterior cervical muscles to monitor the EMG. The frontal EEG, EOG, nuchal EMG and the electrical activity of the LGN were recorded on a Grass polygraph (Model 7). The amplified signals were digitized and stored on a Macintosh G4 computer using a 1320 Digidata A-D card (Instrutech Corporation, New York) and Axograph acquisition software (Axograph Scientific).

Cats were recorded during a) baseline sessions in which the animals were already habituated to the experimental setting, b) control sessions in which bilateral injections of the randomized OD were delivered, and c) antisense sessions in which bilateral injections of the OD directed against cat NGF mRNA were delivered. The solution of the antisense OD or a randomized version of the NGF antisense (2-5 nmols in 1 μl of phosphate buffered saline, PBS) were injected bilaterally into an area of the ponto-mesencephalic tegmentum that encompasses portions of the LDT-PPT (P 0 to −1.5, L 2 to 3, H -2.5 to -4, according to Berman's atlas using a 2 μl Hamilton microsyringe (Berman, 1968). This region of the LDT-PPT contains a large number of cholinergic cells (Jones and Beaudet, 1987). It should be noted that, in the cat, there is a partial overlap of catecholaminergic neurons of the locus coeruleus with cholinergic neurons in the LDT-PPT (Jones and Beaudet, 1987). However, because the overlapping of cholinergic and catecholaminergic cells principally occurs in areas caudal to P −2 (ibid.), the antisense OD centered in a region in which catecholaminergic neurons are scarce. OD injections in each side of the brainstem were conducted sequentially, separated by a ten minutes period of time; the injection of the 1 μl OD solution was completed in a period of 15 minutes.

Five cats received one series of antisense OD injections; each series consisted of bilateral injections delivered in three to six consecutive days. Three of these cats received, in addition to the antisense OD, an identical series of control, randomized OD. Antisense OD and randomized OD series of injections were separated by, at least, 7 days. In each daily session, recording was begun after a period of one hour in which the animal was either undisturbed with the door of the chamber open (baseline session) or being bilaterally injected with the control or antisense ODs (control and antisense sessions, respectively). All control and antisense OD injections were completed by 10:00; baseline, control, and antisense sessions lasted approximately 6 hours (from 10:00 to 16:00, approximately, during the lights-on period of the day).

In two animals, a second antisense OD microinjections series was performed. These series were truncated at the third day (peak of the antisense-induced effects). The animals were euthanized 3 hours later in order to see the effect on the antisense OD on NFG-like immunoreactivity. The FITC-labeled, randomized, control OD was also injected in these animals 21 hours prior to euthanasia. This FITC-labeled OD was visualized in mesopontine sections that were immunostained for NGF and ChAT (see below). In these animals the location of the FITC-labeled OD confirmed that the injections series targeted the LDT-PPT (see Figure 7). In the rest of the animals we verified that the injections series targeted the LDT-PPT, by visualization of the cannula track in selected sections.

4.4. Perfusion and Fixation

Under deep anesthesia induced by Nembutal (20 mg/kg, i.v.), the cats were perfused transcardially with 1.5 l of heparinized saline, followed by 4% paraformaldehyde, 15% saturated picric acid, 0.25 glutaraldehyde, in 0.1M PB (pH 7.4). The brainstem was removed and post-fixed overnight in 2% paraformaldehyde, 7.5% saturated picric acid in 0.1M PB with 10% sucrose. It was then blocked and cryo-protected in 25% sucrose in 0.1M PB. Thereafter, brainstem blocks were serially sectioned on a Reichart-Jung cryostat at a thickness of 14 to 25 μm.

4.5. Immunohistochemical procedures

Immunohistochemical studies to determine the presence of NGF and ChAT in the LDT-PPT were conducted in brainstem tissue that was obtained from three naïve and two antisense OD-injected cats.

NGF-like immunostaining—NGF-like immunoreactivity was visualized using bright field and immunofluorescence microscopic techniques. For fluorescence immunostaining, the free-floating sections were rinsed four times during a period of 25 min, followed by a 60 min blocking step using 10% normal donkey serum (NDS). The sections were then incubated for two days (the first day at 4°C and then moved to room temperature) with constant gentle rotation in 0.1 M PBS - 0.2% Triton ×100 (PBST) – 0.1% Na azide - 6% NDS with anti-NGF (#AB1528sp, Chemicon International, Temecula, California) at a dilution of 1:300. The sections were then rinsed for a period of 25 min in PBST, followed by a 3-hr incubation in donkey anti-sheep rhodamine Red-X with 3% bovine serum albumin (BSA) in PBST at a dilution of 1:100. Thereafter, the sections were rinsed in PBST, mounted onto Superfrost Plus slides (VWR International) and coverslipped using Vectashield mounting media (Vector Laboratories, Burlingame, CA).

For bright field microscopy visualization of NGF immunostaining, free-floating sections were pretreated with 0.3% H_2O_2 PBS for 30 min. The sections were rinsed four times during a period of 25 min, which was followed by a blocking step using 10% normal donkey serum in PBST for 60 min. Next, they were incubated for two days (the first day at 4°C and then moved to room temperature) with gentle rotation in 0.1 M PBS - 0.1% Na azide - 6%NDS with anti-NGF (#sc-548, Santa Cruz Biotechnology, Santa Cruz, CA or #AB1528sp, Chemicon International, Temecula, CA) at 1:500. After rinsing in PBST, the tissue was incubated for 90 minutes in a biotinylated donkey anti-rabbit IgG at a 1:300 dilution (Jackson Laboratories, West Grove, PA). The sections were then rinsed in PBST and treated with the ABC complex (Vector standard Elite kit; Vector Laboratories, Burlingame, CA) at a dilution of 1:200 for 60 min. After another rinsing, peroxidase activity was visualized by the DAB method, as previously described (Yamuy et al., 1998). Control procedures are specified in the Results section.

ChAT immunostaining—The same brainstem sections that were processed for NGF bright field visualization were rinsed five times during a period of 30 minutes, followed by a blocking step using 10% NDS for 60 min. They were then incubated for 72 hours (48 hours at 4 degrees and the last 24 hours at room temperature) with gentle rotation in PBST - 0.1% Na azide - 3% NDS with an antibody directed against ChAT (Chemicon International, Temecula, CA) diluted at 1:400. The sections were rinsed several times in PBST and placed, for 3 hr, into a fluorescent secondary IgG (obtained from Jackson Immunoresearch, West Grove, PA). A donkey IgG raised against rabbit conjugated to Rhodamine Red-X was used at a concentration of 1:100. The sections were rinsed several times in PBST, mounted onto Superfrost Plus slides (VWR International), and coverslipped using Vectashield mounting

media (Vector Laboratories, Burlingame, CA). We have utilized the same methodology and antibodies in previous studies (Yamuy et al., 1995b; Torterolo et al., 2001).

4.6. Data analysis

The anatomical studies focused on NGF, ChAT, and the fluorescein-tagged control OD labeling in neurons in the LDT-PPT. Specifically, we examined, in coronal brainstem sections, the following region of the pontine reticular formation: rostro-caudally, from P 0 to P -1.5 (Berman, 1968); mediolaterally, from the lateral border of the raphe dorsalis to L 5 (ibid.); and dorsoventrally, from the floor of the fourth ventricle to a horizontal plane passing through the middle of the pontine tegmentum (ibid.). In this region, the area circumscribed by cholinergic cells was globally considered as part of the LDT-PPT.

Bright field photomicrographs were taken with a Photometrics CoolSnap *CF* camera attached to a Nikon Eclipse 80*i* Microscope. Photomicrographs captured under fluorescence conditions were taken with a Photometrics CoolSnap *ES* camera also attached to the Nikon Eclipse 80*i*. Adequate filters were used for visualization of FITC and rhodamine fluorescence. The images were digitized and stored with MetaMorph software (A.G. Heinze Precision MicroOptics, CA) and saved on a Dell PC computer. Images were then prepared for presentation using commercial imaging software (Adobe PhotoShop and Adobe Illustrator).

Polygraphic recordings were used to score records of behavioral states and to construct hypnograms using previously described criteria to define the states of sleep and wakefulness (Yamuy et al., 1995a).

In order to determine whether antisense-induced effects were significant, data were taken from baseline sessions, and from all days of each control OD and antisense OD series of injections.

The results are presented as means ± the standard error of the mean (SEM). The level of statistical significance between the mean values of the time spent in different behavioral states that were obtained from paired, control and antisense OD injections within each animal was evaluated using the two-tailed paired Student's *t* test (the results of 15 antisense OD and the correspondent 15 control OD microinjection were paired in 3 cats). For multiple comparisons, multifactorial ANOVA, followed by Scheffé *post hoc* tests, were used (5 cats, see Table 1). The Scheffé test is robust and does not require the assumption of equal variance, normal distribution, or equal sample size. In all statistical tests, the criterion chosen to discard the null hypothesis was set at $P < 0.05$.

We also examined the possibility that the antisense OD altered the frequency components of the EEG that are typical for each behavioral state. Using fast Fourier transforms (FFT, developed for the Axograph software), the power of frequencies between 0 and 60 Hz were determined for the frontal EEG. Accordingly, FFT of 5 artifact-free samples, 10 s in duration each, were obtained during quiet wakefulness, deep NREM sleep and REM sleep from representative baseline (5 cats; 75 samples in total), control antisense (3 cats; 45 samples in total), and antisense (5 cats; 75 samples in total) recording sessions. The samples selected for the antisense microinjections were from the recording day in which the maximal effect on REM sleep was evident. To evaluate differences in the EEG power spectrum, confidence interval tests that are included in the Axograph software were employed.

Acknowledgments

Supported by USPHS grant MH59284. The authors thank Trent Wenzel for his excellent technical assistance.

References

Auld DS, Mennicken F, Quirion R. Nerve growth factor rapidly induces prolonged acetylcholine release from cultured basal forebrain neurons: differentiation between neuromodulatory and neurotrophic influences. J Neurosci. 2001; 21:3375–3382. [PubMed: 11331367]

Barclay J, Patel S, Dorn G, Wotherspoon G, Moffatt S, Eunson L, Abdel'al S, Natt F, Hall J, Winter J, Bevan S, Wishart W, Fox A, Ganju P. Functional downregulation of P2X3 receptor subunit in rat sensory neurons reveals a significant role in chronic neuropathic and inflammatory pain. J Neurosci. 2002; 22:8139–8147. [PubMed: 12223568]

Berman, AL. The brain stem of the cat A citoarchitectonic atlas with stereotaxic coordinates. University of Wisconsin; Madison: 1968.

Borbely AA. A two process model of sleep regulation. Hum Neurobiol. 1982; 1:195–204. [PubMed: 7185792]

Clements JR, Grant S. Glutamate-like immunoreactivity in neurons of the laterodorsal tegmental and pedunculopontine nuclei in the rat. Neurosci Lett. 1990; 120:70–73. [PubMed: 2293096]

Curro Dossi R, Pare D, Steriade M. Short-lasting nicotinic and long-lasting muscarinic depolarizing responses of thalamocortical neurons to stimulation of mesopontine cholinergic nuclei. J Neurophysiol. 1991; 65:393–406. [PubMed: 2051187]

Datta S, Spoley EE, Patterson EH. Microinjection of glutamate into the pedunculopontine tegmentum induces REM sleep and wakefulness in the rat. Am J Physiol Regulatory Integrative Comp Physiol. 2001; 280:R752–R759.

el Mansari M, Sakai K, Jouvet M. Responses of presumed cholinergic mesopontine tegmental neurons to carbachol microinjections in freely moving cats. Exp Brain Res. 1990; 83:115–123. [PubMed: 2073933]

Ettaiche M, Deval E, Cougnon M, Lazdunski M, Voilley N. Silencing acid-sensing ion channel 1a alters cone-mediated retinal function. J Neurosci. 2006; 26:5800–5809. [PubMed: 16723538]

Fuller PM, Saper CB, Lu J. The pontine REM switch: past and present. J Physiol. 2007; 584:735–741. [PubMed: 17884926]

Hallanger AE, Wainer BH. Ascending projections from the pedunculopontine tegmental nucleus and the adjacent mesopontine tegmentum in the rat. J Comp Neurol. 1988; 274:483–515. [PubMed: 2464621]

Heumann R, Schwab M, Merkl R, Thoenen H. Nerve growth factor-mediated induction of choline acetyltransferase in PC12 cells: evaluation of the site of action of nerve growth factor and the involvement of lysosomal degradation products of nerve growth factor. J Neurosci. 1984; 4:3039–3050. [PubMed: 6502222]

Jacobs JS, Miller MW. Expression of nerve growth factor, p75, and the high affinity neurotrophin receptors in the adult rat trigeminal system: evidence for multiple trophic support systems. J Neurocytol. 1999; 28:571–595. [PubMed: 10800206]

Jia HG, Yamuy J, Sampogna S, Morales FR, Chase MH. Colocalization of gamma-aminobutyric acid and acetylcholine in neurons in the laterodorsal and pedunculopontine tegmental nuclei in the cat: a light and electron microscopic study. Brain Res. 2003; 992:205–219. [PubMed: 14625059]

Jones, B. Basic mechanisms of sleep-wake states. In: Kryger, MH., et al., editors. Principles and practices of sleep medicine. Elsevier-Saunders; Philadelphia: 2005. p. 136-153.

Jones BE. Immunohistochemical study of choline acetyltransferase-immunoreactive processes and cells innervating the pontomedullary reticular formation in the rat. J Comp Neurol. 1990; 295:485–514. [PubMed: 2351765]

Jones BE. Paradoxical REM sleep promoting and permitting neuronal networks. Arch Ital Biol. 2004; 142:379–396. [PubMed: 15493543]

Jones BE, Beaudet A. Distribution of acetylcholine and catecholamine neurons in the cat brainstem: a choline acetyltransferase and tyrosine hydroxylase immunohistochemical study. J Comp Neurol. 1987; 261:15–32. [PubMed: 2887593]

Kawai H, Zago W, Berg DK. Nicotinic alpha 7 receptor clusters on hippocampal GABAergic neurons: regulation by synaptic activity and neurotrophins. J Neurosci. 2002; 22:7903–7912. [PubMed: 12223543]

Knipper M, Leung LS, Zhao D, Rylett RJ. Short-term modulation of glutamatergic synapses in adult rat hippocampus by NGF. Neuroreport. 1994; 5:2433–2436. [PubMed: 7696574]

Knusel B, Hefti F. Development of cholinergic pedunculopontine neurons in vitro: comparison with cholinergic septal cells and response to nerve growth factor, ciliary neuronotrophic factor, and retinoic acid. J Neurosci Res. 1988; 21:365–375. [PubMed: 3216429]

Lauterborn JC, Isackson PJ, Gall CM. Cellular localization of NGF and NT-3 mRNAs in postnatal rat forebrain. Mol Cell Neurosci. 1994; 5:46–62. [PubMed: 8087414]

Leonard CS, Llinas R. Serotonergic and cholinergic inhibition of mesopontine cholinergic neurons controlling REM sleep: an in vitro electrophysiological study. Neuroscience. 1994; 59:309–330. [PubMed: 8008195]

Leonetti JP, Mechti N, Degols G, Gagnor C, Lebleu B. Intracellular distribution of microinjected antisense oligonucleotides. Proc Natl Acad Sci U S A. 1991; 88:2702–2706. [PubMed: 1849273]

Lohof AM, Ip NY, Poo MM. Potentiation of developing neuromuscular synapses by the neurotrophins NT-3 and BDNF. Nature. 1993; 363:350–353. [PubMed: 8497318]

Luppi PH, Gervasoni D, Verret L, Goutagny R, Peyron C, Salvert D, Leger L, Fort P. Paradoxical (REM) sleep genesis: The switch from an aminergic-cholinergic to a GABAergic-glutamatergic hypothesis. Journal of Physiology (Paris). 2007; 100:271–283.

Luther JA, Birren SJ. Nerve growth factor decreases potassium currents and alters repetitive firing in rat sympathetic neurons. J Neurophysiol. 2006; 96:946–958. [PubMed: 16707716]

Maisonpierre PC, Belluscio L, Friedman B, Alderson RF, Wiegand SJ, Furth ME, Lindsay RM, Yancopoulos GD. NT-3, BDNF, and NGF in the developing rat nervous system: parallel as well as reciprocal patterns of expression. Neuron. 1990; 5:501–509. [PubMed: 1688327]

McCarley RW. Mechanisms and models of REM sleep control. Arch Ital Biol. 2004; 142:429–467. [PubMed: 15493547]

McCarley RW. Neurobiology of REM and NREM sleep. Sleep Med. 2007; 8:302–330. [PubMed: 17468046]

Mitani A, Ito K, Hallanger AE, Wainer BH, Kataoka K, McCarley RW. Cholinergic projections from the laterodorsal and pedunculopontine tegmental nuclei to the pontine gigantocellular tegmental field in the cat. Brain Res. 1988; 451:397–402. [PubMed: 3251602]

Nishio T, Furukawa S, Akiguchi I, Oka N, Ohnishi K, Tomimoto H, Nakamura S, Kimura J. Cellular localization of nerve growth factor-like immunoreactivity in adult rat brain: quantitative and immunohistochemical study. Neuroscience. 1994; 60:67–84. [PubMed: 8052420]

Pare D, Smith Y, Parent A, Steriade M. Projections of brainstem core cholinergic and non-cholinergic neurons of cat to intralaminar and reticular thalamic nuclei. Neuroscience. 1988; 25:69–86. [PubMed: 3393287]

Quartu M, Geic M, Del Fiacco M. Neurotrophin-like immunoreactivity in the human trigeminal ganglion. Neuroreport. 1997; 8:3611–3617. [PubMed: 9427336]

Quartu M, Serra MP, Manca A, Follesa P, Lai ML, Del Fiacco M. Neurotrophin-like immunoreactivity in the human pre-term newborn, infant, and adult cerebellum. Int J Dev Neurosci. 2003; 21:23–33. [PubMed: 12565693]

Sala R, Viegi A, Rossi FM, Pizzorusso T, Bonanno G, Raiteri M, Maffei L. Nerve growth factor and brain-derived neurotrophic factor increase neurotransmitter release in the rat visual cortex. Eur J Neurosci. 1998; 10:2185–2191. [PubMed: 9753104]

Semba K, Fibiger HC. Afferent connections of the laterodorsal and the pedunculopontine tegmental nuclei in the rat: a retro- and antero-grade transport and immunohistochemical study. J Comp Neurol. 1992; 323:387–410. [PubMed: 1281170]

Semba K, Reiner PB, Fibiger HC. Single cholinergic mesopontine tegmental neurons project to both the pontine reticular formation and the thalamus in the rat. Neuroscience. 1990; 38:643–654. [PubMed: 2176719]

Shen RY, Altar CA, Chiodo LA. Brain-derived neurotrophic factor increases the electrical activity of pars compacta dopamine neurons in vivo. Proc Natl Acad Sci U S A. 1994; 91:8920–8924. [PubMed: 8090745]

Shiromani PJ, Floyd C, Velazquez-Moctezuma J. Pontine cholinergic neurons simultaneously innervate two thalamic targets. Brain Res. 1990; 532:317–322. [PubMed: 2282524]

Siegel, JM. REM Sleep. In: Kryger, MH., et al., editors. Principles and practices of sleep medicine. Elsevier-Saunders; Philadelphia: 2005. p. 120-135.

Skinner RD, Homma Y, Garcia-Rill E. Arousal mechanisms related to posture and locomotion: 2. Ascending modulation. Prog Brain Res. 2004; 143:291–298. [PubMed: 14653173]

Steriade M. Arousal: revisiting the reticular activating system. Science. 1996; 272:225–226. [PubMed: 8602506]

Steriade, M. Brain electrical activity and sensory processing during waking and sleep states. In: Kryger, MH., et al., editors. Principles and practices of sleep medicine. Saunders; Philadelphia: 2005. p. 101-119.

Steriade M, Datta S, Pare D, Oakson G, Curro Dossi RC. Neuronal activities in brain-stem cholinergic nuclei related to tonic activation processes in thalamocortical systems. J Neurosci. 1990; 10:2541–2559. [PubMed: 2388079]

Steriade M, Dossi RC, Nunez A. Network modulation of a slow intrinsic oscillation of cat thalamocortical neurons implicated in sleep delta waves: cortically induced synchronization and brainstem cholinergic suppression. J Neurosci. 1991a; 11:3200–3217. [PubMed: 1941080]

Steriade M, Dossi RC, Pare D, Oakson G. Fast oscillations (20-40 Hz) in thalamocortical systems and their potentiation by mesopontine cholinergic nuclei in the cat. Proc Natl Acad Sci U S A. 1991b; 88:4396–4400. [PubMed: 2034679]

Thakkar MM, Ramesh V, Cape EG, Winston S, Strecker RE, McCarley RW. REM sleep enhancement and behavioral cataplexy following orexin (hypocretin)-II receptor antisense perfusion in the pontine reticular formation. Sleep Res Online. 1999; 2:113–120.

Thakkar MM, Winston S, McCarley RW. A1 receptor and adenosinergic homeostatic regulation of sleep-wakefulness: effects of antisense to the A1 receptor in the cholinergic basal forebrain. J Neurosci. 2003; 23:4278–4287. [PubMed: 12764116]

Torterolo P, Vanini G. New concepts in relation to generating and maintaining arousal. Rev Neurol. 2010; 50:747–758. [PubMed: 20533253]

Torterolo P, Yamuy J, Sampogna S, Morales FR, Chase MH. GABAergic neurons of the laterodorsal and pedunculopontine tegmental nuclei of the cat express c-fos during carbachol-induced active sleep. Brain Res. 2001; 892:309–319. [PubMed: 11172778]

Ure DR, Campenot RB. Retrograde transport and steady-state distribution of 125I-nerve growth factor in rat sympathetic neurons in compartmented cultures. J Neurosci. 1997; 17:1282–1290. [PubMed: 9006972]

Wahlestedt C, Golanov E, Yamamoto S, Yee F, Ericson H, Yoo H, Inturrisi CE, Reis DJ. Antisense oligodeoxynucleotides to NMDA-R1 receptor channel protect cortical neurons from excitotoxicity and reduce focal ischaemic infarctions. Nature. 1993; 363:260–263. [PubMed: 8487863]

Wang X, Butowt R, Vasko MR, von Bartheld CS. Mechanisms of the release of anterogradely transported neurotrophin-3 from axon terminals. J Neurosci. 2002; 22:931–945. [PubMed: 11826122]

Webster HH, Jones BE. Neurotoxic lesions of the dorsolateral pontomesencephalic tegmentum-cholinergic cell area in the cat. II. Effects upon sleep-waking states. Brain Res. 1988; 458:285–302. [PubMed: 2905197]

Xi MC, Morales FR, Chase MH. Evidence that wakefulness and REM sleep are controlled by a GABAergic pontine mechanism. J Neurophysiol. 1999; 82:2015–2019. [PubMed: 10515993]

Yamuy, J.; Borde, M.; Chase, MH. Modulation of the activity of pontine reticular neurons by nerve growth factor (NGF). Proceedings of the Society for Neuroscience; San Diego. 2004. p. 546.5

Yamuy J, Mancillas JR, Morales FR, Chase MH. C-fos expression in the pons and medulla of the cat during carbachol- induced active sleep. J Neurosci. 1993; 13:2703–2718. [PubMed: 8501533]

Yamuy J, Morales FR, Chase MH. Induction of rapid eye movement sleep by the microinjection of nerve growth factor into the pontine reticular formation of the cat. Neuroscience. 1995a; 66:9–13. [PubMed: 7637879]

Yamuy J, Ramos O, Torterolo P, Sampogna S, Chase MH. The role of tropomyosin-related kinase receptors in neurotrophin-induced rapid eye movement sleep in the cat. Neuroscience. 2005; 135:357–369. [PubMed: 16125858]

Yamuy J, Rojas MJ, Torterolo P, Sampogna S, Chase MH. Induction of rapid eye movement sleep by neurotrophin-3 and its co-localization with choline acetyltransferase in mesopontine neurons. Neuroscience. 2002; 115:85–95. [PubMed: 12401324]

Yamuy J, Sampogna S, Chase MH. Neurotrophin-receptor immunoreactive neurons in mesopontine regions involved in the control of behavioral states. Brain Res. 2000; 866:1–14. [PubMed: 10825475]

Yamuy J, Sampogna S, Lopez-Rodriguez F, Luppi PH, Morales FR, Chase MH. Fos and serotonin immunoreactivity in the raphe nuclei of the cat during carbachol-induced active sleep: a double-labeling study. Neuroscience. 1995b; 67:211–223. [PubMed: 7477901]

Yamuy, J.; Sampogna, S.; Morales, FR.; Chase, MH. c-fos expression in mesopontine noradrenergic and cholinergic neurons of the cat during carbachol-induced active sleep: A double labeling study; Sleep Res Online. 1998. p. 28-40.http://www.sro.org/1998/Yamuy/1928/

Abbreviations

ANOVA	analyses of variance
ARAS	ascending reticular activating system
ChAT	choline acetyltransferase
DAB	diaminobenzidine
EEG	electroencephalogram
EMG	electromyogram
EOG	electro-oculogram
FITC	fluorescein isothiocyanate
FFT	fast Fourier transforms
LDT	laterodorsal tegmental nucleus
LGN	lateral geniculate nucleus
NDS	normal donkey serum
NGF	nerve grown factor
NPO	nucleus pontis oralis
NREM	non-REM
NT-3	neurotrophin 3
OD	oligodeoxyribonucleotide
PBS	phosphate buffered saline
PBST	PBS plus triton
PGO	ponto-geniculo-occipital
PPT	pedunculo-pontine tegmental nucleus
REM	rapid-eye movement
SEM	standard error of the mean
SWA	slow wave activity
trkA	tropomyosin-related kinase A

Highlights

- Mesopontine cholinergic neurons of the cat exhibit NGF-like immunoreactivity.
- Blockade of NGF production in the LDT-PPT reduces REM sleep time.
- Blockade of NGF production in the LDT-PPT increases wakefulness
- Our data strongly suggests that NGF is involved in sleep regulation.

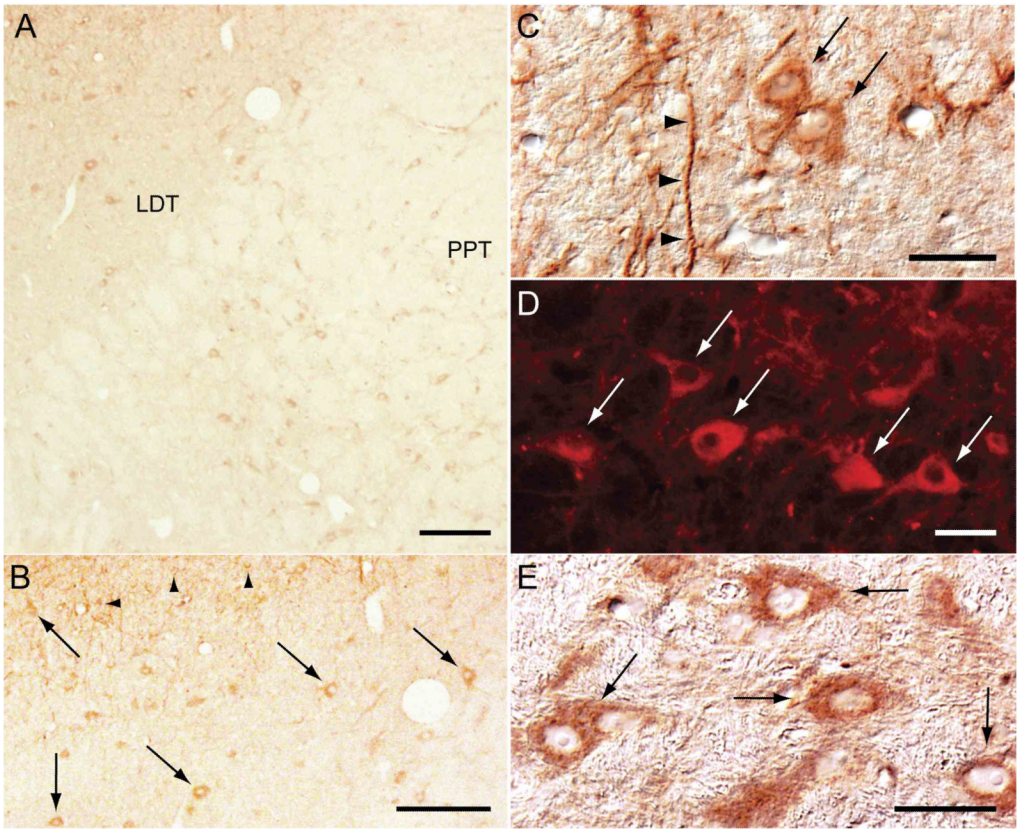

Figure 1.

NGF immunoreactivity is present in neurons in the LDT and PPT of the cat. A large number of NGF immunoreactive neurons were distributed throughout a region of the pontine tegmentum that encompasses the LDT and PPT (A). These neurons were medium to large in size (20-40 μm in soma diameter) and round, fusiform, or multipolar in shape in both the LDT (arrows in B, C, and D) and the PPT (E). NGF immunoreactive dendritic processes were present throughout the LDT-PPT (arrowheads in C). Scattered in the LDT, particularly in its periaqueductal portion, were small-sized cells, probably glia, that also exhibited NGF immunoreactivity (arrowheads in B). NGF immunoreactivity was visualized using the DAB method for bright-field microscopy (A, B, C, and E) or immunofluorescence techniques (D, rhodamine). Calibration bars A and B, 200 μm; C, D and E, 40 μm.

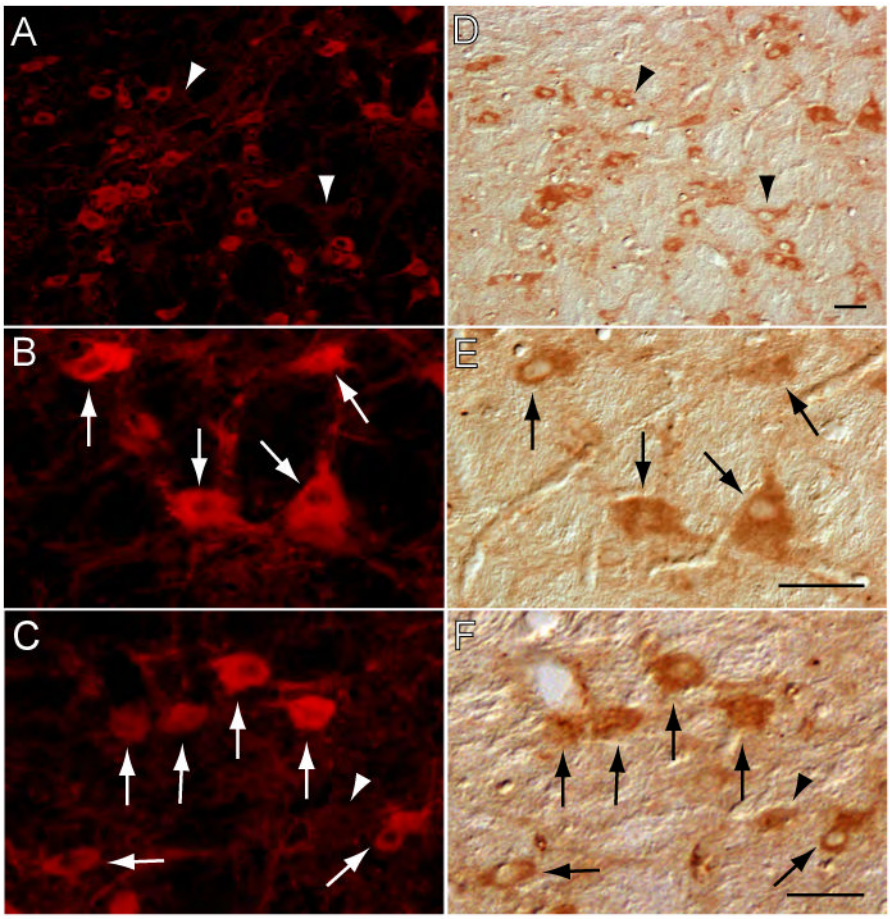

Figure 2.
Cholinergic neurons in the LDT and PPT contain NGF. Neurons in the LDT that exhibited choline acetyltransferase (ChAT) immunoreactivity (A), also showed NGF immunostaining (D). A subset of these ChAT+, NGF+ neurons is depicted in B and E, at a larger magnification. A similar co-localization of ChAT and NGF was observed in the PPT (C and F). Note, however, that not all NGF-containing cells were immunostained for ChAT (NGF single-labeled cells indicated by arrowheads in A and D). The photomicrographs in A-E were taken from a single pontine section that was stained for ChAT (rhodamine) and NGF (DAB method). The photomicrographs in C and F were obtained from another single pontine section that was treated similarly. Calibration bars, 40 μm.

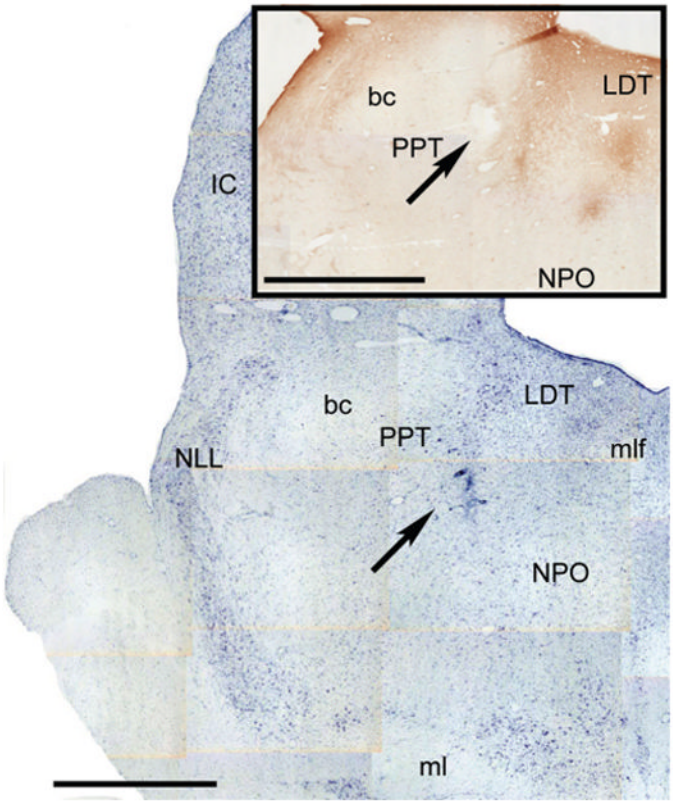

Figure 3.
Microinjetion site of a representative antinsense OD microinjection. The Figure depicts two nearby hemisections counterstained with Nissl and immunostained for NGF (inset) of a representative animal. The arrows indicate the microinjection site. Calibration bars: 2 mm.

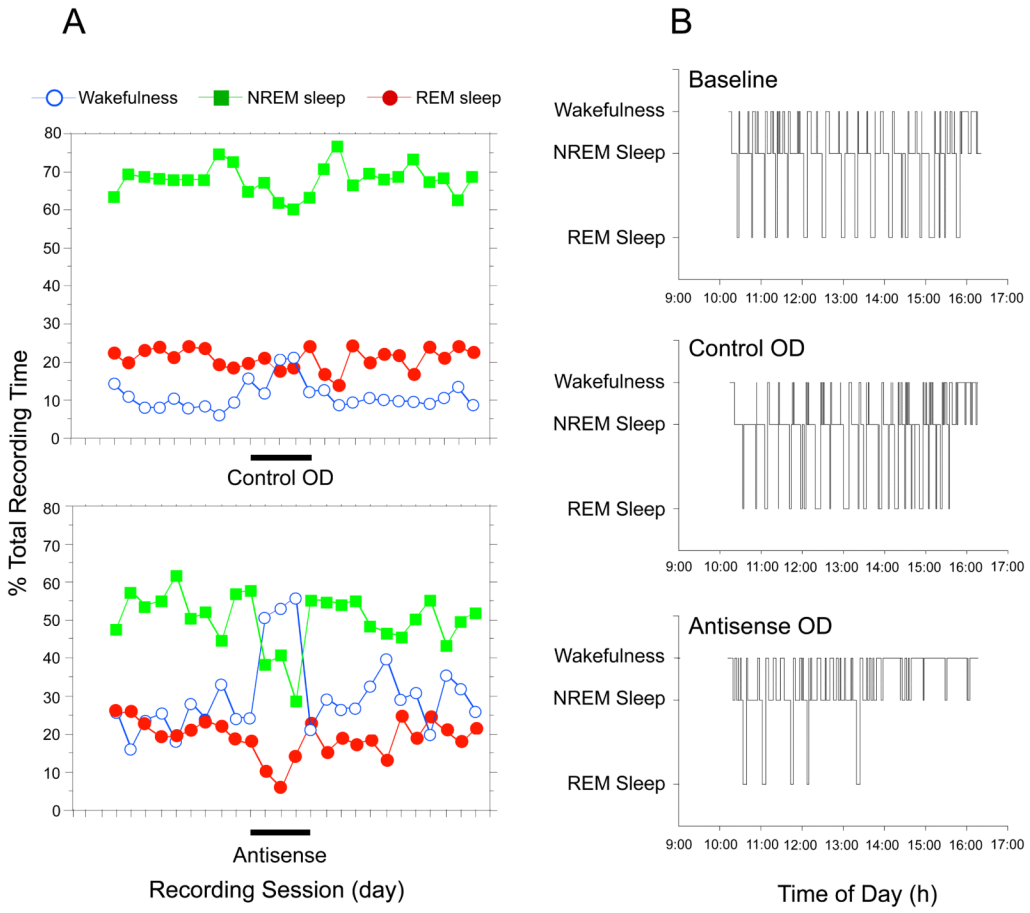

Figure 4.

The microinjection into the LDT-PPT of an antisense oligodeoxynucleotide (OD) directed against NGF cat mRNA produces changes in sleep and wakefulness. The charts in A illustrate the relative time spent in each behavioral state during daily recording sessions without injections (baseline), with control OD injections (control OD) and antisense OD injections (antisense). This cat received a series of five control and antisense OD injections that were delivered in consecutive days (marked by the bars in the abscissa in the upper and lower charts in A). The control and antisense OD series were separated by 25 days. Hypnograms taken from a representative baseline session and from the third day of control and antisense OD injections depict the alterations in sleep and wakefulness cycle that typically occurred during antisense OD sessions (B).

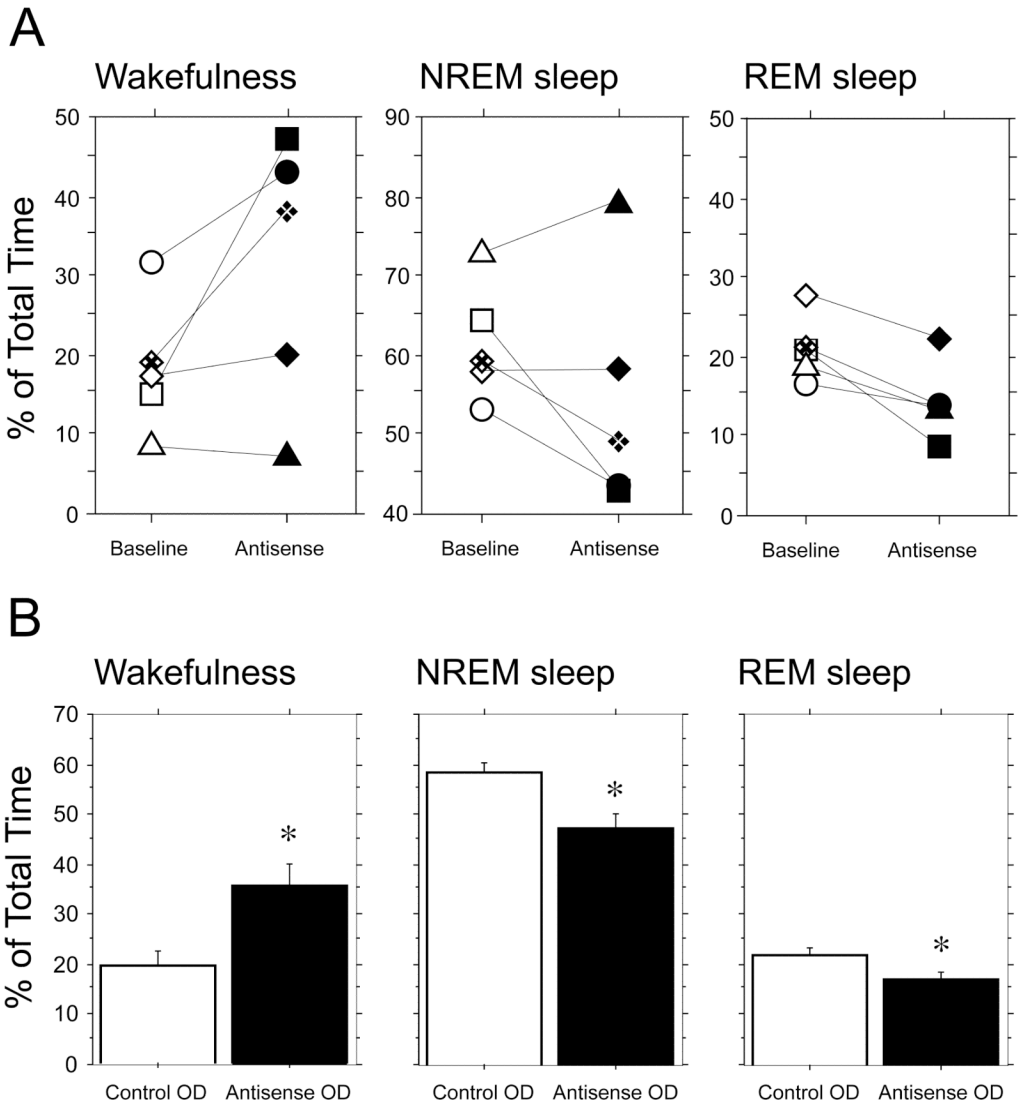

Figure 5.

The antisense oligodeoxynucleotide (OD) injections into the dorsolateral mesopontine tegmentum produced significant changes in the states of sleep and wakefulness. The mean percentage time spent in wakefulness, NREM sleep, and REM sleep pooled from each series of antisense OD sessions (filled symbols in A, each symbol represents the mean value obtained from one animal) were different than those obtained from representative baseline sessions (empty symbols in A). Note that the mean time spent in REM sleep decreased during antisense OD sessions in all cases. However, because the antisense OD changes were manifest during the second or third day of injection, the effects are likely underestimated (see charts in Fig. 4A). The data in A were obtained from five cats, which were injected with the antisense OD. The mean percentage of time spent in wakefulness, NREM sleep, and REM sleep during the recording sessions in which a randomized control antisense or an antisense OD were microinjected into the LDT-PPT are illustrated in B. Compared to the control OD (empty bars in B), the antisense OD produced an increase in wakefulness and a decrease in NREM sleep and REM sleep (solid bars in B). The difference in the means for the three behavioral states was statistically significant according to the paired t test (wakefulness, $P = 0.0017$, NREM sleep, $P = 0.0045$; REM sleep, $P = 0.0028$; n = 15). As

indicated for the charts in A, because the effect of the NGF antisense exhibited a delay of at least one day and data from all injection recording sessions were included, the difference in the means for all states are likely underestimated. The data in B were obtained from three cats that were injected with both the control and antisense ODs in series that consisted of five microinjections each, delivered on five consecutive days. Control and antisense OD series of injections in each animal were separated by at least one week. For further details, see Methods and Results.

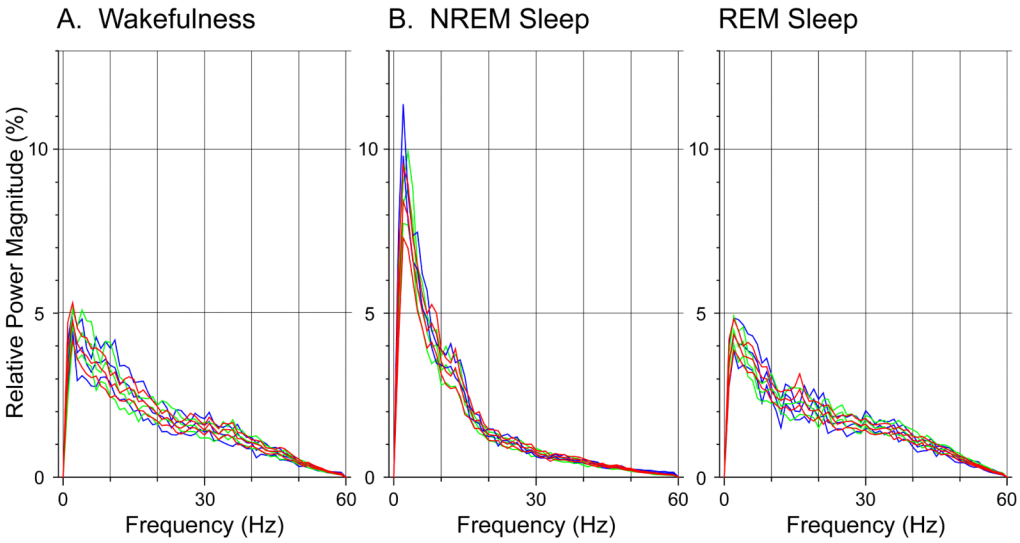

Figure 6.

The EEG power spectrum is not altered following antisense OD administration. The mean frequency distribution obtained from frontal EEG recordings during wakefulness, NREM sleep, and REM sleep (A, B, and C, respectively) were similar, i.e., the confidence intervals overlapped, for baseline, control OD, and antisense OD recording sessions (indicated by green, blue and red line curves, respectively). Each curve is the mean power spectrum pooled from five representative, 10 second episodes of each behavioral state that were obtained from representative baseline (5 cats), control OD (3 cats), and antisense OD (5 cats) recording sessions.

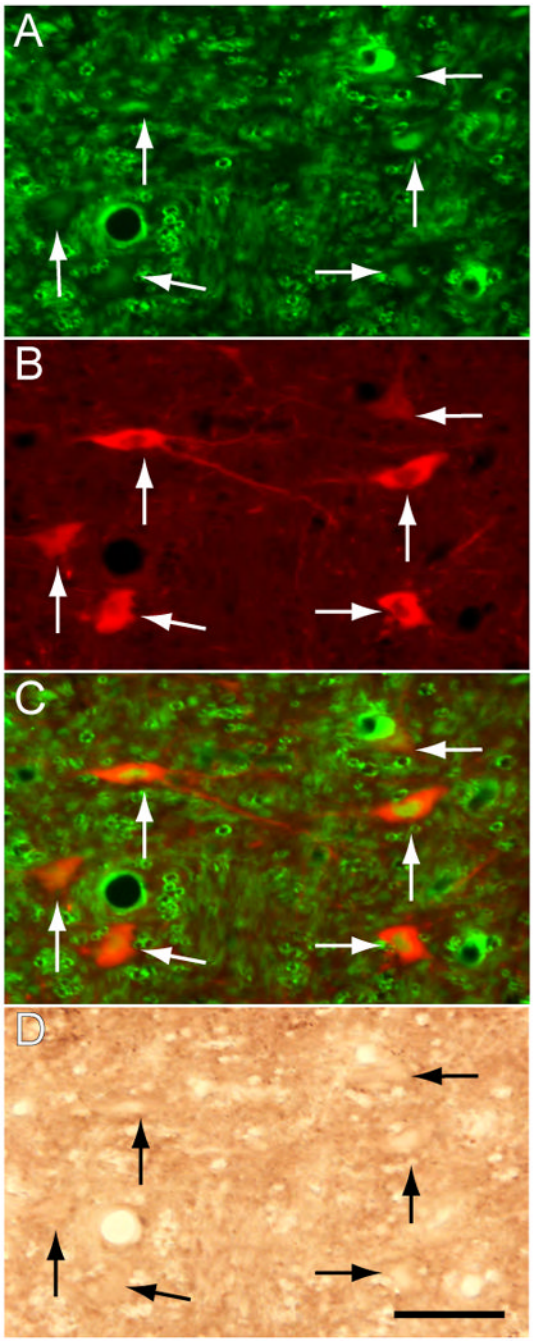

Figure 7.

The antisense OD blocks the production of NGF within the region of injection in the LDT-PPT. An FITC-labeled control antisense was microinjected 18 hours prior to the last antisense OD injection, which preceded euthanasia by approximately 3 hours (see Methods). The FITC-labeled OD was taken up by neurons in the LDT that exhibit immunofluorescent nuclei and cytoplasms (arrows in A). A subpopulation of FITC-labeled neurons are ChAT immunoreactive, i.e., cholinergic in nature (B and the merged image of A and B, in C). The identical field in the LDT shows that these cholinergic cells are devoid of NGF immunoreactivity (D). ChAT immunolabeling was processed with rhodamine; NGF immunoreactivity was visualized with the DAB method. Calibration mark, 40 μm.

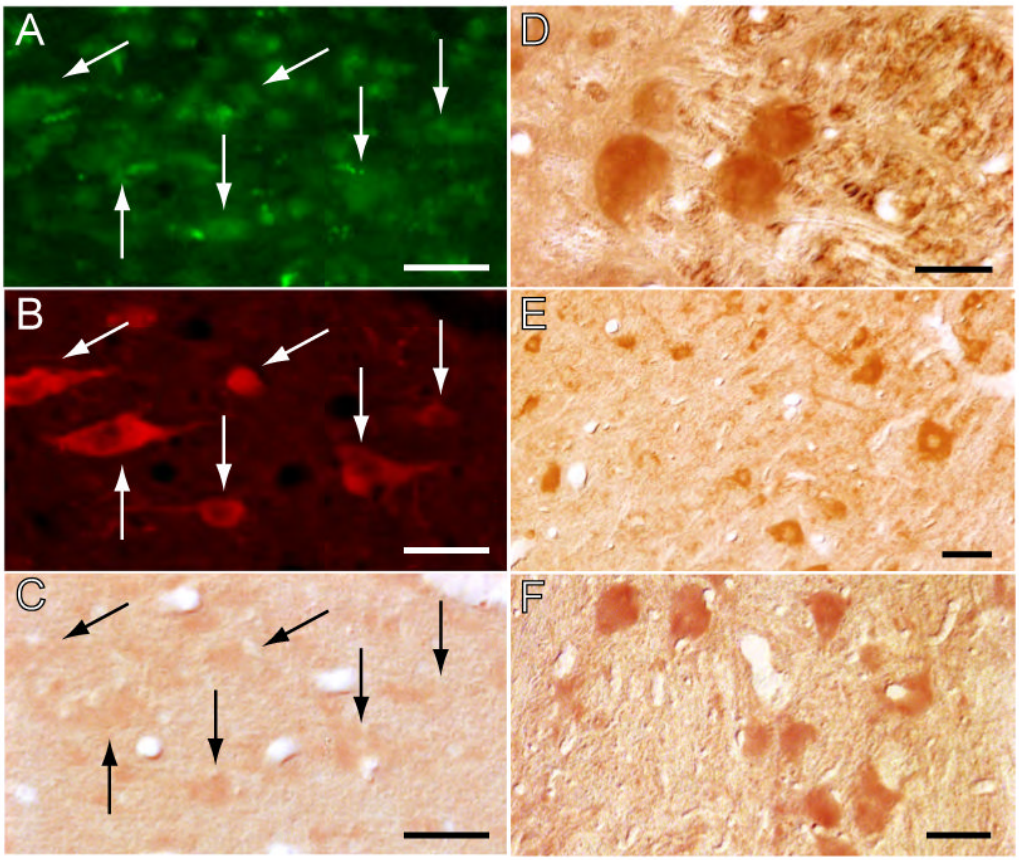

Figure 8.

The blockade of NGF production is restricted to the site of antisense OD injections. The antisense was taken up by neurons in the LDT of a cat that was injected with an FITC-labeled control antisense into the same area where the antisense OD was applied (arrows in A); the immunolabeled neurons included a contingent of ChAT-containing cells (arrows in B). These cholinergic neurons exhibited only faint NGF immunoreactivity (arrows in C). In contrast, in nuclei more distant to the antisense OD injection, neurons were strongly immunoreactive for NGF (mesencephalic trigeminal nucleus, D; cochlear nucleus, E; and vestibular complex, F). ChAT immunolabeling was processed for rhodamine visualization; NGF immunoreactivity was visualized with the DAB method. Calibration marks, A-C, 40 μm; D, E and F, 30 μm.

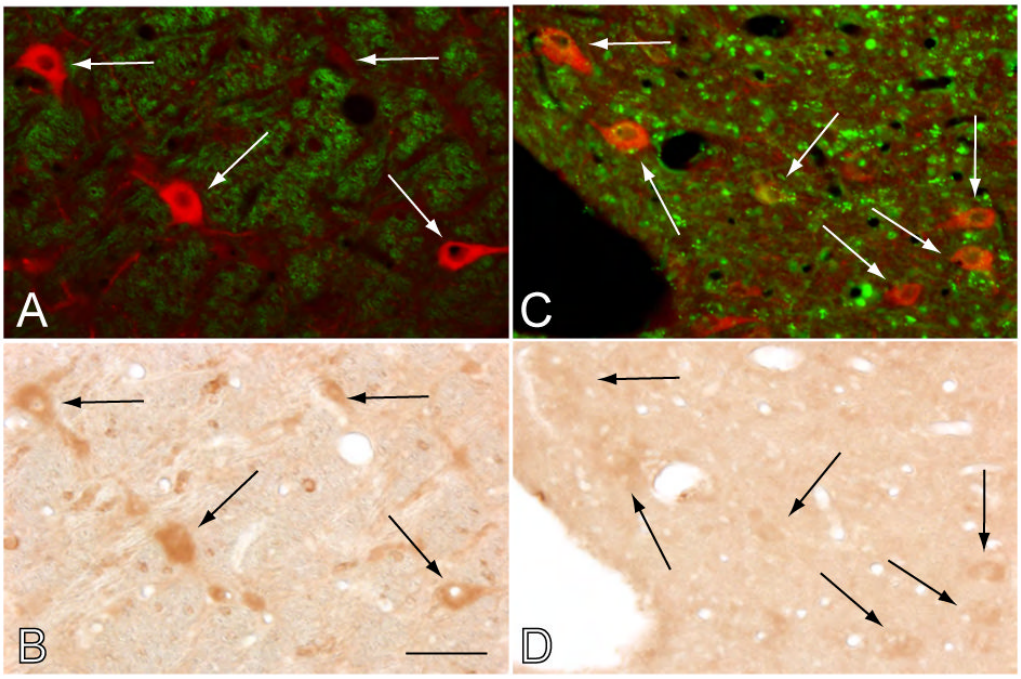

Figure 9.

The blockade of NGF production occurs within and in the vicinity of the antisense OD injection site in the latero-dorsal and pedunculo-pontine tegmental (LDT and PPT) nuclei. A portion of the PPT that lacks the FITC-labeled control OD, located approximately 1 mm anterior to the site of antisense OD application, shows ChAT-containing neurons (indicated by arrows in A; merged image wherein ChAT is visualized in red and FITC in green). The same cells exhibit strong NGF immunoreactivity (arrows in B). A site adjacent to the injection of antisense OD, in the same animal, shows extra- and intracellular granular, FITC-labeled, accumulations of the fluorescein-tagged control OD injected prior to euthanasia. Some of the neurons at the site of antisense injection that took up the antisense OD were cholinergic (arrows in C; merged image in which ChAT is visualized in red and FITC in green). The same cholinergic cells in the injection site were virtually devoid of NGF immunoreactivity (arrows in D). ChAT immunolabeling was processed with rhodamine; NGF immunoreactivity was visualized with the DAB method. Calibration mark, 40 μm.

Table 1

Changes in sleep and wakefulness that occurred following the microinjection of an antisense oligodeoxynucleotide into the LDT-PPT region of the cat brainstem.

	Baseline	Control OD	Antisense OD
Time Spent in Wakefulness (%)	17.2 ± 0.01	20.0 ± 0.03	30.9 ± 0.04****,†
Time Spent in NREM Sleep (%)	61.7 ± 0.01	57.7 ± 0.02	54.2 ± 0.03*
Time Spent in REM Sleep (%)	21.0 ± 0.004	22.4 ± 0.01	14.9 ± 0.01****,†††
NREM Sleep Latency (min.)	1.1 ± 0.18	1.9 ± 0.50	4.0 ± 1.37***
REM Sleep Latency (min.)	17.0 ± 1.15	12.9 ± 2.07	27.3 ± 4.26**,††
Wake Episodes per hour	4.7 ± 0.12	4.9 ± 0.49	4.1 ± 0.35
NREM Sleep Episodes per hour	5.3 ± 0.13	5.4 ± 0.52	4.5 ± 0.35
REM Sleep Episodes per hour	2.4 ± 0.08	2.3 ± 0.20	1.6 ± 0.12****,†
Wake Episodes Duration (min.)	2.3 ± 0.15	2.7 ± 0.42	5.6 ± 1.15****,††
NREM Sleep Episodes Duration (min.)	7.5 ± 0.25	7.1 ± 0.55	7.7 ± 0.10
REM Sleep Episodes Duration (min.)	5.7 ± 0.18	6.5 ± 0.65	5.6 ± 0.45

Values are means ± SEM. The data were obtained from 100 baseline sessions, 15 control OD sessions and 27 antisense OD sessions, which were conducted in five cats. The asterisks represent the level of statistical difference between the means of antisense OD sessions vs. baseline and control OD sessions based on multifactorial ANOVA and the Scheffé *post hoc* test (differences between the means of baseline vs. control OD sessions were not present); the crosses (†) indicate the presence of significant differences between control OD and antisense OD sessions.

$^{*}P < 0.03$;

$^{**}P < 0.001$;

$^{***}P < 0.0005$;

$^{****}P < 0.0001$.

$^{\dagger}P < 0.03$;

$^{\dagger\dagger}P < 0.01$;

$^{\dagger\dagger\dagger}P < 0.0001$.